Solution structure of natively assembled yeast ribosomal stalk determined by Small Angle X-ray Scattering

[*]Przemyslaw Grela, [†‡]Michal J. Gajda, [§]Jean-Paul Armache, [§]Roland Beckmann, [*]Dawid Krokowski, [†]Dmitri I. Svergun, [*]Nikodem Grankowski and [*]Marek Tchorzewski

[*]Department of Molecular Biology, Maria Curie-Sklodowska University, Akademicka 19, 20-033 Lublin, Poland

[†]European Molecular Biology Laboratory, Hamburg Outstation, Notkestrasse 85, 22603 Hamburg, Germany

[§]Gene Center, Department of Biochemistry, Ludwig-Maximilians-Universität München, Feodor-Lynen-Strasse 25, 81377 Munich, Germany

[‡]Max-Planck Karl Bonhoeffer Institute for Biophysical Chemistry, Am Faßberg 11, 37077 Göttingen

Corresponding author. Marek Tchorzewski, Department of Molecular Biology, Maria Curie-Sklodowska University, Akademicka 19, 20-033 Lublin, Poland; Tel. +48 81 537 59 56, e-mail: maro@hektor.umcs.lublin.pl

Short title: Yeast ribosomal stalk structure

Synopsis

The ribosomal stalk of the 60S subunit has been shown to play a crucial role in all steps of protein synthesis, but its structure and exact molecular function remain an open question. In the current study, we present the low resolution models of the solution structure of the yeast ribosomal stalk, composed of five proteins, P0-(P1-P2)2. The model of the pentameric stalk complex determined by small angle X-ray scattering reveals an elongated shape with a maximum length of 13 nm. The model displays three distinct lobes, which may correspond to the individual P1-P2 heterodimers anchored to the C-terminal domain of P0 protein.

Keywords: Ribosome; Ribosomal stalk; Ribosomal P proteins, SAXS, GTPase center, cryo-EM

Introduction

At all stages of protein synthesis the ribosome requires protein factors, known as translational GTPases (tGTPases), which act as molecular switches cycling between active GTP-bound conformation and inactive GDP-form, conferring unidirectionality and fidelity on the translational apparatus. The platform for the tGTPases called GTPase associated region (GAR) is located on the large ribosomal subunit, and is responsible for their activation [1]. The major part of GAR is composed of a set of proteins which form the stalk, responsible for the recruitment of tGTPases and stimulation of factor-dependent GTP hydrolysis [2, 3]. In bacteria, this complex occurs in two configurations: pentameric L10-$(L12)_4$ in mesophiles and heptameric L10-$(L12)_6$ in thermophiles [2, 4]. In archaeal/eukaryotic ribosomes the stalk is heptameric L10-$(L12)_6$ or pentameric P0-$(P1\text{-}P2)_2$, respectively [5-7]. The bacterial/eukaryotic L10/P0 proteins form the base of the stalk interacting with rRNA. The rRNA-binding domain of these proteins is homologous and functionally interchangeable [8]. In turn, the L12/P1-P2 proteins form the functional part of the stalk, attached to the ribosome through the L10/P0 proteins, as $(L12)_2$ or P1-P2 dimers [2, 9-11]. An interesting case is found in lower eukaryotes, such as the yeast *Saccharomyces cerevisiae*, where the two P1/P2 proteins have evolved up to four different proteins, P1A, P1B, P2A and P2B [10, 12]. In contrast to L10/P0, the L12/P1-P2 proteins are regarded as analogous [13]. In spite of the wealth of ribosomal structures determined by crystallography or cryo-EM, the studies of the whole stalk remain poorly established. In the cryo-EM analyses of bacterial/eukaryotic ribosomes, the stalk was only visible as a residual structure representing only its small part [14, 15]. For the bacterial ribosome, the cryo-EM analysis only allowed a fragment of the L12 protein to be located: its C-terminal part was trapped close to the G' domain of EF-G [16]. Also crystallography of ribosomes did not cast more light on the whole stalk. Fragments of L10 protein were visualized, either on the ribosome as rRNA binding domain [2, 17] or as fragments of individual L10 proteins [2, 18]. Also crystallographic analyses of isolated stalk complexes of L10-L12 from bacteria or archaea brought fragmentary information about the stalk architecture, showing the core structure excluding the functional C-terminal domains of L12 (CTD) [2, 19]. An insight into the CTD structure was obtained by NMR [20], crystallography [21, 22] or SAXS [23] analyses. Recently, the stalk was visualized on the bacterial ribosome crystallized in complex with elongation factor G. Maps at a lower

resolution (5.0 Å) allowed placement of L10 and four copies of the N-terminal domain of L12 in the model as polyalanine chains, showing for the first time a substantial fragment of the stalk on the ribosome [24].

We report the low resolution structural model of the yeast ribosomal stalk determined by Small Angle X-ray Scattering (SAXS). The structure encompasses P0 fragment (residues 199-312) with two P1-P2 heterodimers (described in yeast as two independent P1A-P2B and P1B-P2A dimers) representing the entire stalk including the C-termini of P-proteins which constitute the functional part of the stalk. The structure was modeled onto the ribosomal particle, giving the first insight into complete architecture of the ribosome with the stalk.

Experimental

Sample preparation. Preparation of yeast 80S ribosomal particles and stalk complexes was done as described previously [6]. Protein concentration was measured according to Bradford's method using a Bio-Rad protein assay kit, or by optical density at 280 nm using an extinction coefficient calculated from the amino acid composition [25]. Two P-protein complexes were purified: TH199 and TH230 with composition $\Delta P0_{199\text{-}312}$-(P1A-P2B)-(P1B-P2A) and $\Delta P0_{230\text{-}312}$-(P1B-P2A), respectively.

Small Angle X-ray Scattering

Scattering experiments. The synchrotron radiation X-ray scattering data from solutions of the ribosomal stalk complexes were collected on the X33 beamline of the EMBL on the storage ring DORIS III (DESY, Hamburg, Germany). For each complex, several solute concentrations in the range from 1.0 to 15 mg/ml were measured. To monitor for radiation damage, two successive two-minute exposures of protein solutions were compared and no significant changes were observed. The data were normalized to the intensity of the transmitted beam and radially averaged; the scattering of the buffer was subtracted and the difference curves were scaled for protein concentration. The low angle data measured at lower protein concentrations were extrapolated to infinite dilution and merged with the higher concentration data to yield the final composite scattering curves. The data processing steps were performed using the program package PRIMUS [26]. The forward scattering I(0) and the radius of gyration R_g were evaluated using the Guinier approximation [27] assuming that at very small angles ($s<1.3/R_g$) the intensity is represented as $I(s) = I(0) \exp(-(sR_g)2/3)$. These parameters were also cross-checked with the values computed from the entire scattering patterns using the indirect transform package GNOM [28], providing also the pair distribution function of the particle p(r) and the maximum size D_{max}. The excluded volume of the hydrated particle was computed from the small angle portion of the data ($s<3.0$ nm^{-1}) using the equation as described previously. Prior to this analysis an appropriate constant was subtracted from each data point to force the s^{-4} decay of the intensity at higher angles following the Porod's law for homogeneous particles [29].

***Ab initio* shape determination.** The "shape scattering" curves were further used to generate low resolution *ab initio* shapes of the pentameric (TH199) and trimeric (TH230) stalk complexes by DAMMIN [30]. A dozen DAMMIN runs were performed to check the stability of solution, and the results were superimposable with each other. These models were averaged to determine common structural features and to select the most typical shapes using the programs DAMAVER [31] and SUPCOMB [32].

Fitting the stalk structure into ribosomal cryo-EM maps

For visualization of a ribosome stalk model the EMDB database (EMDataBank.org) was screened in search for maps containing strong stalk occupancy. The cryo-EM density maps of 80S particles from *Saccharomyces cerevisiae* (EMD-1668)[33] and *Canis familiaris* (EMD-1480)[34] were selected. They were aligned in UCSF Chimera [35] and filtered to 10 Å. A simulated density map of *S. cerevisiae* ribosome at 10 Å was created from pdb files (3IZB 3IZF 3IZE and 3IZS) [36] using VMD program [37]. The stalk P-proteins (P0, P1/P2) were simulated separately from pdb using the Surface option in the UCSF Chimera program.

Results and discussion

SAXS parameters. One of the major obstacles for the high resolution analysis of the stalk is its dynamic nature [11, 38], which hampers crystallographic and cryo-EM analyses. The use of NMR is hindered by the size of the complex, which usually exceeds 50 kDa; and preparation of the complex is challenging as three or five [in yeast, P0-(P1A-P2B)-(P1B-P2A)] components have to be tightly assembled. To bring insight into the stalk structure, we employed SAXS, which provides low resolution data only but overcomes the limitations of the other methods. The stalk was obtained from *S. cerevisiae* ribosomal particles, employing procedure, which allowed isolation of natively assembled complexes [6]. Two complexes were used: pentameric TH199, having a truncated P0 protein with the rRNA-binding domain removed and only the P-domain left intact (residues 199-312), able to bind the two independent P1A-P2B and P1B-P2A dimers; and the trimeric TH230, $\Delta P0_{230\text{-}312}$-(P1B-P2A), which is a further deletion form of the TH199 complex containing a truncated variant of P0 able to bind only one dimer, P1B-P2A. Both complexes were subjected to SAXS analysis yielding the processed experimental data in Fig. 1A. The Guiner plots (Fig. 1A, inset) were linear, suggesting that the protein complexes form monodisperse solutions containing single molecular species. The estimated molecular mass of the pentameric complex (55 ±7 kDa) agrees with the value calculated from the primary sequence (56.42 kDa). For the truncated variant, the experimental value of 40±6 kDa exceeded the calculated value (31.18 kDa). However, the excluded particle volume of the truncated variant (Fig.1B) scaled well with that of the full complex indicating that the truncated complex is not aggregated. The distance distribution functions p(r) of the complexes (Fig. 1A) are bell-shaped functions typical for globular particles. The distribution of the TH199 complex is more skewed pointing to an elongated particle with a cross-section of about 2.5 nm (corresponding to the maximum of the p(r)). The trimeric TH230 displays a more symmetrical p(r) function and reveals the same maximum diameter (13 nm) as the truncated variant suggesting that the TH230 'folds back' into TH199 complex.

Overall structure determination. Low-resolution models of the TH199 and TH230 complexes were reconstructed *ab initio* from the experimental scattering patterns. The obtained models of the two complexes provide good fits to the experimental data (Fig. 1A). The TH199 structure has a flattened anisometric elongated shape with three domains, belonging presumably to the individual dimers and to the ΔP0 (Fig. 1C). The model of the TH230 complex reflects part of the TH199 pentamer lacking one domain (Fig. 1D). These relationships are visualized by aligning the two structures (Fig. 2). TH230 can be fitted into the TH199 complex (Fig. 2B), showing that the missing domain corresponds to the P1A-P2B dimer. The relative position of the P1A/P2B dimer was verified by aligning the model of

TH199 complex with the structural model of the P1A-P2B dimer previously determined by SAXS [23]. The fitting of the dimer within the pentamer (Fig. 2A) showed that P1A-P2B occupies the edge of the stalk. The location of the dimer was also confirmed by rebuilding the framework of the TH199 pentamer using TH230 and the P1A-P2B dimer (Fig. 2C). Therefore, the architecture of the stalk can be visualized as two dimers arranged in parallel, brought into contact by their respective interaction with the P0. As it has been shown for the stalk from *P. horikoshii*, the individual dimers are attached to P0 by its helical spine [19] and are arranged one after the other on P0. However, the archaeal structure lacks the C-termini of the P-proteins and represents the core of the stalk, in contrast to the present SAXS model. Given the low resolution of the present model, the P1/P2 C-termini cannot be located unequivocally, but a tentative assignment of the C-terminal part of P0 can be made. Considering that the P-domain of P0 protein forms the helical spine responsible for binding of the dimers, we propose that helices are located in the main body of the SAXS structure, and the protruding structure may correspond to the flexible C-terminus, forming a distinctive beak (Fig. 2).

Modelling of the stalk complex on the 80S ribosome. Knowing the position of the stalk on the ribosome may help understand the actions of the GAR. Using the above model of the stalk we built a complete picture of the eukaryotic ribosome (Fig. 3). In the cryo-EM data of eukaryotic ribosomes the stalk is missing [36] or is represented by a residual structure [39], and based on homology to the bacterial structures, this which can be assigned to the helical spine of L10 protein and the core of the L12 dimers [2]. Also, in recent crystallographic analysis of the yeast ribosome the stalk is visible as residual fragment represented by fragment of P0 protein (residue 3-107; 182-221) and two P1A/P2B proteins (residue 1-46 and 5-51, respectively) [40]. As it was discussed, the main obstacle in stalk visualization is its dynamic nature, which also hamper analyses by cryo-EM, the technique also sensitive to structural fluctuations. Considering cryo-EM, a structure of a complex is a result of averaging the information from all the individual particles taken for analysis. This is good for alignable stable parts, such as the core of the ribosomal large subunit, where it brings more detail. However, an averaging of the stalk in multiple positions results in the observed smudge and lack of high-resolution features. The farther away from the stabilized protein-RNA interaction of the stalk base P0/L10 protein, the less information is available, therefore the resolution of the whole stalk in the absence of a stabilizing factor is highly unlikely, especially the C-terminal domains which are considered unstructured. Therefore, in all cryo-EM reconstructions of the 80S ribosome or 60S subunit, the stalk represent undescribed entity, and it should be underlined, that this is the largest ribosomal element to escape from the structural characterization on the ribosomal particle.

Since this particular element of the stalk is structurally conserved between bacterial and archaeal/eukaryotic, as shown by the recent structure of an archeal stalk complex [19], it is likely that the eukaryotic structure visible on cryo-EM maps belongs to the same structural entity. Therefore, the EMDB database was screened for maps containing the strongest stalk occupancy, and the *S. cerevisiae* [33] and *C. familiaris* [34] cryo-EM density maps were chosen (Fig. 3). After filtering down to 10 Å resolution, they were aligned with the present stalk SAXS model. Additionally, a simulated density map of *S. cerevisiae* ribosome at 10 Å was created from pdb files (3IZB 3IZF 3IZE and 3IZS) using VMD program (Fig. 3B). Initial inspection suggested that the stalk visible in all densities is a sufficient size to accommodate the SAXS model. The latter can be fitted into the cryo-EM density at the extended stalk region in both maps, (Fig 3A and C). In order to locate precisely the stalk elements, we

reconstructed this structure using several individual components. We took the bacterial and archeal L10 rRNA-binding domain [2, 17]. Additionally, the mode of L10-L12 interaction was built based on structures in a non-ribosomal state of archeal P0-P1 from *P. horikoshii* [19] and P0 from *M. jannaschii* [18]. These structures complement each other, as the *P. horikoshii* structure represents the rRNA-binding domain and the C-terminal domain of P0, with fragments of P1 dimers, while *M. jannaschii* data comprises rRNA-binding domain and domain II, characteristic element for Archeal/Eukaryotic P0, but lacks P1/P2 termini. By combining those structures we constructed a stalk model on the yeast cryo-EM ribosome (Fig 3B). The model was aligned with the stalk SAXS structure. The protruding part of the reconstituted model fits with the solution stalk structure. In our model, the C-termini of P1/P2 proteins face outward. The single C-terminus of P0 (beak) in SAXS model protrudes from the reconstituted model and represents its continuation. However, as we have proposed for the bacterial L12 protein [38], the yeast P1/P2 C-termini, having a flexible hinge, may sample a large volume to efficiently recruit translation factors or RIP proteins [41]. Therefore, our SAXS model and its proposed ribosomal location represent single steady-state conformational position.

Author Contribution

Przemyslaw Grela, Michal J. Gajda, Jean-Paul Armache performed the experiments and collected the data; Roland Beckmann, Dmitri I. Svergun, helped with interpretation of the data; Dawid Krokowski prepared yeast strains, helped with data interpretation; Marek Tchorzewski designed the experiment, interpreted the data and wrote the manuscript.

Funding

This work was supported by the Ministry of Science and Higher Education, Poland grant nr N302 061034. D.S. acknowledges support from the BMBF Research Grant SYNC-LIFE (contract number 05K10YEA).

The authors declare that they have no conflict of interest.

References

1 Clementi, N. and Polacek, N. (2010) Ribosome-associated GTPases: the role of RNA for GTPase activation. RNA Biol. **7**, 521-527

2 Diaconu, M., Kothe, U., Schlunzen, F., Fischer, N., Harms, J. M., Tonevitsky, A. G., Stark, H., Rodnina, M. V. and Wahl, M. C. (2005) Structural Basis for the Function of the Ribosomal L7/12 Stalk in Factor Binding and GTPase Activation. Cell. **121**, 991-1004

3 Huang, C., Mandava, C. S. and Sanyal, S. (2010) The ribosomal stalk plays a key role in IF2-mediated association of the ribosomal subunits. J Mol Biol. **399**, 145-153

4 Ilag, L. L., Videler, H., McKay, A. R., Sobott, F., Fucini, P., Nierhaus, K. H. and Robinson, C. V. (2005) Heptameric (L12)6/L10 rather than canonical pentameric complexes

are found by tandem MS of intact ribosomes from thermophilic bacteria. Proc Natl Acad Sci U S A. **102**, 8192-8197

5 Maki, Y., Hashimoto, T., Zhou, M., Naganuma, T., Ohta, J., Nomura, T., Robinson, C. V. and Uchiumi, T. (2007) Three binding sites for stalk protein dimers are generally present in ribosomes from archaeal organism. J Biol Chem. **282**, 32827-32833

6 Grela, P., Krokowski, D., Gordiyenko, Y., Krowarsch, D., Robinson, C. V., Otlewski, J., Grankowski, N. and Tchorzewski, M. (2010) Biophysical properties of the eukaryotic ribosomal stalk. Biochemistry. **49**, 924-933

7 Guarinos, E., Santos, C., Sanchez, A., Qiu, D. Y., Remacha, M. and Ballesta, J. P. (2003) Tag-mediated fractionation of yeast ribosome populations proves the monomeric organization of the eukaryotic ribosomal stalk structure. Mol Microbiol. **50**, 703-712

8 Uchiumi, T., Hori, K., Nomura, T. and Hachimori, A. (1999) Replacement of L7/L12.L10 protein complex in Escherichia coli ribosomes with the eukaryotic counterpart changes the specificity of elongation factor binding. J Biol Chem. **274**, 27578-27582

9 Grela, P., Sawa-Makarska, J., Gordiyenko, Y., Robinson, C. V., Grankowski, N. and Tchorzewski, M. (2008) Structural properties of the human acidic ribosomal P proteins forming the P1-P2 heterocomplex. J Biochem. **143**, 169-177

10 Guarinos, E., Remacha, M. and Ballesta, J. P. (2001) Asymmetric interactions between the acidic P1 and P2 proteins in the Saccharomyces cerevisiae ribosomal stalk. J Biol Chem. **276**, 32474-32479

11 Mulder, F. A., Bouakaz, L., Lundell, A., Venkataramana, M., Liljas, A., Akke, M. and Sanyal, S. (2004) Conformation and dynamics of ribosomal stalk protein L12 in solution and on the ribosome. Biochemistry. **43**, 5930-5936

12 Krokowski, D., Tchorzewski, M., Boguszewska, A. and Grankowski, N. (2005) Acquisition of a stable structure by yeast ribosomal P0 protein requires binding of P1A-P2B complex: in vitro formation of the stalk structure. Biochim Biophys Acta. **1724**, 59-70

13 Grela, P., Bernado, P., Svergun, D., Kwiatowski, J., Abramczyk, D., Grankowski, N. and Tchorzewski, M. (2008) Structural relationships among the ribosomal stalk proteins from the three domains of life. J Mol Evol. **67**, 154-167

14 Agrawal, R. K., Penczek, P., Grassucci, R. A. and Frank, J. (1998) Visualization of elongation factor G on the Escherichia coli 70S ribosome: the mechanism of translocation. Proc Natl Acad Sci U S A. **95**, 6134-6138

15 Gomez-Lorenzo, M. G., Spahn, C. M., Agrawal, R. K., Grassucci, R. A., Penczek, P., Chakraburtty, K., Ballesta, J. P., Lavandera, J. L., Garcia-Bustos, J. F. and Frank, J. (2000) Three-dimensional cryo-electron microscopy localization of EF2 in the Saccharomyces cerevisiae 80S ribosome at 17.5 A resolution. Embo J. **19**, 2710-2718

16 Datta, P. P., Sharma, M. R., Qi, L., Frank, J. and Agrawal, R. K. (2005) Interaction of the G' domain of elongation factor G and the C-terminal domain of ribosomal protein L7/L12 during translocation as revealed by cryo-EM. Mol Cell. **20**, 723-731

17 Kavran, J. M. and Steitz, T. A. (2007) Structure of the base of the L7/L12 stalk of the Haloarcula marismortui large ribosomal subunit: analysis of L11 movements. J Mol Biol. **371**, 1047-1059

18 Kravchenko, O., Mitroshin, I., Nikonov, S., Piendl, W. and Garber, M. (2010) Structure of a two-domain N-terminal fragment of ribosomal protein L10 from Methanococcus jannaschii reveals a specific piece of the archaeal ribosomal stalk. J Mol Biol. **399**, 214-220

19 Naganuma, T., Nomura, N., Yao, M., Mochizuki, M., Uchiumi, T. and Tanaka, I. (2010) Structural basis for translation factor recruitment to the eukaryotic/archaeal ribosomes. J Biol Chem. **285**, 4747-4756

20 Bocharov, E. V., Sobol, A. G., Pavlov, K. V., Korzhnev, D. M., Jaravine, V. A., Gudkov, A. T. and Arseniev, A. S. (2004) From structure and dynamics of protein L7/L12 to molecular switching in ribosome. J Biol Chem. **279**, 17697-17706

21 Leijonmarck, M. and Liljas, A. (1987) Structure of the C-terminal domain of the ribosomal protein L7/L12 from Escherichia coli at 1.7 A. J Mol Biol. **195**, 555-579

22 Wahl, M. C., Bourenkov, G. P., Bartunik, H. D. and Huber, R. (2000) Flexibility, conformational diversity and two dimerization modes in complexes of ribosomal protein L12. Embo J. **19**, 174-186

23 Grela, P., Helgstrand, M., Krokowski, D., Boguszewska, A., Svergun, D., Liljas, A., Bernado, P., Grankowski, N., Akke, M. and Tchorzewski, M. (2007) Structural characterization of the ribosomal P1A-P2B protein dimer by small-angle X-ray scattering and NMR spectroscopy. Biochemistry. **46**, 1988-1998

24 Gao, Y. G., Selmer, M., Dunham, C. M., Weixlbaumer, A., Kelley, A. C. and Ramakrishnan, V. (2009) The structure of the ribosome with elongation factor G trapped in the posttranslocational state. Science. **326**, 694-699

25 Gill, S. C. and von Hippel, P. H. (1989) Calculation of protein extinction coefficients from amino acid sequence data. Anal Biochem. **182**, 319-326

26 Konarev, P. V., Volkov, V. V., Sokolova, A. V., Koch, M. H. J. and Svergun, D. I. (2003) PRIMUS - a Windows-PC based system for small-angle scattering data analysis. J. Appl. Crystallogr. **36**, 1277-1282

27 Guinier, A. (1939) La diffraction des rayons X aux tres petits angles; application a l'etude de phenomenes ultramicroscopiques. Ann. Phys. (Paris). **12**, 161-237

28 Svergun, D. I. (1992) Determination of the regularization parameter in indirect transform methods using perceptual criteria. J. Appl. Crystallogr. **25**, 495 - 503

29 Porod, G. (1982) General theory. In Small-Angle X-ray Scattering (Glatter, O. and Kratky, O., eds.). pp. 17-51, Academic Press, New York

30 Svergun, D. I. (1999) Restoring low resolution structure of biological macromolecules from solution scattering using simulated annealing. Biophys J. **76**, 2879-2886

31 Volkov, V. V. and Svergun, D. I. (2003) Uniqueness of ab initio shape determination in small angle scattering. J. Appl. Crystallogr. **36**, 860-864

32 Kozin, M. B. and Svergun, D. I. (2001) Automated matching of high- and low-resolution structural models. J. Appl. Crystallogr. **34**, 33-41

33 Becker, T., Bhushan, S., Jarasch, A., Armache, J. P., Funes, S., Jossinet, F., Gumbart, J., Mielke, T., Berninghausen, O., Schulten, K., Westhof, E., Gilmore, R., Mandon, E. C. and Beckmann, R. (2009) Structure of monomeric yeast and mammalian Sec61 complexes interacting with the translating ribosome. Science. **326**, 1369-1373

34 Chandramouli, P., Topf, M., Menetret, J. F., Eswar, N., Cannone, J. J., Gutell, R. R., Sali, A. and Akey, C. W. (2008) Structure of the mammalian 80S ribosome at 8.7 A resolution. Structure. **16**, 535-548

35 Pettersen, E. F., Goddard, T. D., Huang, C. C., Couch, G. S., Greenblatt, D. M., Meng, E. C. and Ferrin, T. E. (2004) UCSF Chimera--a visualization system for exploratory research and analysis. J Comput Chem. **25**, 1605-1612

36 Armache, J. P., Jarasch, A., Anger, A. M., Villa, E., Becker, T., Bhushan, S., Jossinet, F., Habeck, M., Dindar, G., Franckenberg, S., Marquez, V., Mielke, T., Thomm, M., Berninghausen, O., Beatrix, B., Soding, J., Westhof, E., Wilson, D. N. and Beckmann, R.

(2010) Cryo-EM structure and rRNA model of a translating eukaryotic 80S ribosome at 5.5-A resolution. Proc Natl Acad Sci U S A. **107**, 19748-19753

37 Humphrey, W., Dalke, A. and Schulten, K. (1996) VMD: visual molecular dynamics. J Mol Graph. **14**, 33-38, 27-38

38 Bernado, P., Modig, K., Grela, P., Svergun, D. I., Tchorzewski, M., Pons, M. and Akke, M. (2010) Structure and Dynamics of Ribosomal Protein L12: An Ensemble Model Based on SAXS and NMR Relaxation. Biophys J. **98**, 2374-2382

39 Spahn, C. M., Beckmann, R., Eswar, N., Penczek, P. A., Sali, A., Blobel, G. and Frank, J. (2001) Structure of the 80S ribosome from Saccharomyces cerevisiae--tRNA-ribosome and subunit-subunit interactions. Cell. **107**, 373-386

40 Ben-Shem, A., Garreau de Loubresse, N., Melnikov, S., Jenner, L., Yusupova, G. and Yusupov, M. (2011) The structure of the eukaryotic ribosome at 3.0 A resolution. Science. **334**, 1524-1529

41 Li, X. P., Grela, P., Krokowski, D., Tchorzewski, M. and Tumer, N. E. (2010) Pentameric organization of the ribosomal stalk accelerates recruitment of ricin a chain to the ribosome for depurination. J Biol Chem. **285**, 41463-41471

Figure legends

Fig. 1. The overall SAXS parameters. (A) distance distribution functions p(r) computed from experimental data by GNOM. The inset shows experimental X-ray scattering patterns and scattering computed from their models; (B) parameters computed from experimental data, (MM, Rg, Dmax, denote: molecular masses, radii of gyration, maximum sizes, respectively, χ is the discrepancy between the experimental data and the computed scattering from the most probable GASBOR models); (C) and (D) - *ab initio* models of pentameric TH199 and trimeric TH230 complexes, respectively; models are shown in front view and were generated with the VMD program.

Fig. 2. Alignment of *ab initio* models of the yeast stalk complexes. (A) Superimposition of pentameric TH199 (light grey) with model of dimer P1A-P2B (black); (B) comparison of pentameric (light grey) and trimeric (dark grey) complexes; (C) alignment of all three complexes. Upper panel, front view, lower panels show the structures rotated clockwise by 90^{o} around the X-axis.

Fig. 3. Structure of the stalk complex on 80S ribosome. (A) - *S. cerevisiae* 80S cryo-EM map of ribosome aligned with the stalk SAXS structure added (red); (B) - *S. cerevisiae* 80S cryo-EM map of ribosome, where density from the cryo-EM model of the stalk was replaced by reconstructed stalk structure based on crystallographic data (green), the position of SAXS model is shown in red; (C) *C. familiaris* 80S ribosomal cryo-EM map with the yeast SAXS stalk added. Yellow - small ribosomal subunit, white - large ribosomal subunit, red - SAXS stalk model. The cryo-EM maps were generated with the Chimera program.

A

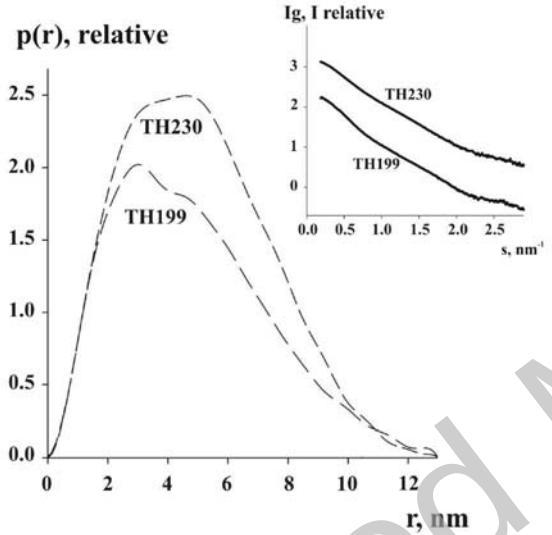

B

Construct	MM (kDa)	R_g(nm)	V_p(nm^3)	D_{max}(nm)	χ
TH230	40±6	3.8±0.2	110±10	13±1	1.3
TH 199	55±7	3.9±0.2	150±15	13±1	1.3

C

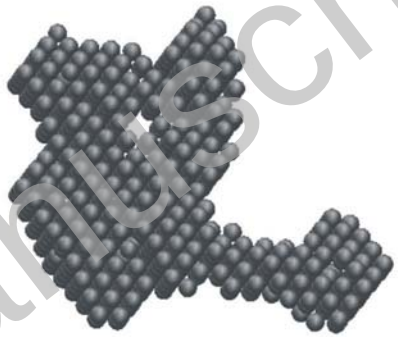

D

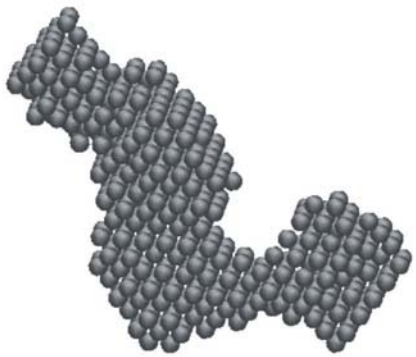

Biochemical Journal Immediate Publication. Published on 29 Mar 2012 as manuscript BJ20120115